Theory and Measurement of Backscattering from RFID Tags

Pavel V. Nikitin and K. V. S. Rao

Intermec Technologies Corporation
6001 36th Ave W, Everett, WA 98203, USA
Tel. +1 (425) 248-2600; E-mail: {pavel.nikitin, kvs.rao}@intermec.com

Abstract

This paper presents a method for measuring signal backscattering from RFID tags, and for calculating a tag's radar cross section (RCS). We derive a theoretical formula for the RCS of an RFID tag with a minimum-scattering antenna. We describe an experimental measurement technique, which involves using a network analyzer connected to an anechoic chamber with and without the tag. The return loss measured in this way allows us to calculate the backscattered power and to find the tag's RCS. Measurements were performed using an RFID tag operating in the UHF band. To determine whether the tag was turned on, we used an RFID tag tester. The tag's RCS was also calculated theoretically, using electromagnetic simulation software. The theoretical results were found to be in good agreement with experimental data.

Keywords: Antenna measurements; radar cross sections; RFID

1. Introduction

Radio-frequency identification (RFID) is a rapidly developing automatic wireless data-collection technology with a long history [1]. The first multi-bit functional passive UHF RFID systems, with a range of several meters, appeared in the early 1970s [2], and continued to evolve through the 1980s [3]. Recently, RFID has experienced a tremendous growth, due to developments in integrated circuits and radios, and due to increased interest from the retail industry and government [4]. RFID UHF bands vary in different countries, and include frequencies between 860 MHz and 960 MHz. The most popular UHF RFID standards are the ISO 18000-6B and the recently ratified EPC Gen2.

There have been numerous publications on antennas for RFID tags (see, e.g., the bibliography in [5]), but only a few works have analyzed the tags' backscattering and radar cross section (RCS) [6-8]. At the same time, there have been several publications on the RCS of linearly and nonlinearly loaded antennas [9-16], not specifically related to RFID. This paper presents a theory and a measurement methodology for determining the RFID tag's RCS. It is an extended version of the conference publication [6].

2. RFID System Operation

Figure 1 illustrates the operation of a passive RFID system, which consists of an RFID tag and a base station, called the "RFID reader." A typical passive tag consists of an antenna and an application-specific integrated circuit (ASIC) chip, both with complex impedances. The chip obtains power from the RF signal transmitted by the RFID reader. The tag sends data back by switching its input impedance between two states and thus modulating the backscattered signal. At each impedance state, the RFID tag presents a certain radar cross section. One of the impedance states is usually high and another is low, to provide a significant difference in the backscattered signal.

The data exchange between the RFID reader and the tag can employ various modulation and coding schemes (e.g., amplitude modulation and Manchester coding). The signal transmitted on the forward link (from the reader to the tag) contains both continuous-wave (CW) and modulated commands, as shown in Figure 2. On the reverse link (from the tag to the reader), the data is sent back during one of the CW periods, when the tag impedance modulates the backscattered signal. More details on RFID system protocol and operation can be found in [17, 18].

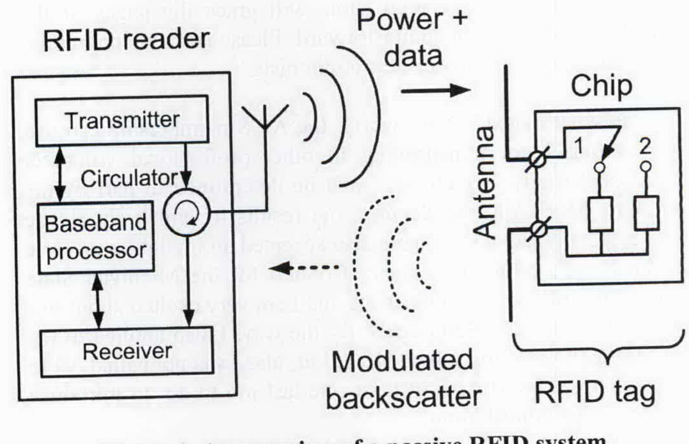

Figure 1. An overview of a passive RFID system.

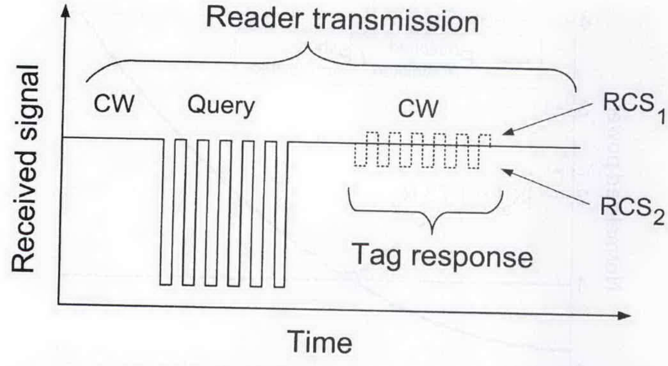

Figure 2. Data exchange between an RFID reader and a tag.

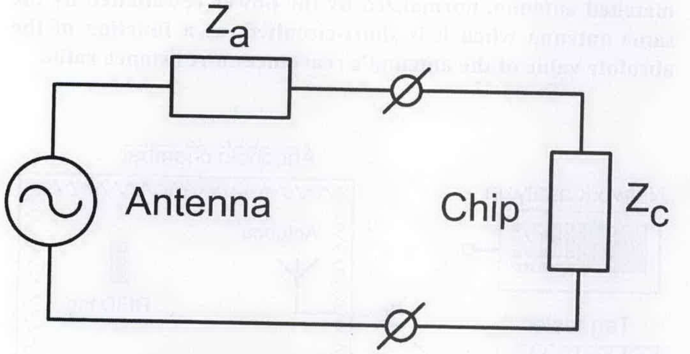

Figure 3. The equivalent circuit of an RFID tag.

3. Impedance Matching of an RFID Tag

A proper impedance match between the antenna and the chip is very important in RFID. It directly influences the RFID system's performance characteristics, such as the range of a tag: the maximum distance at which a reader can either read or write information to the tag.

In RFID tags, the antenna is usually directly connected to the chip, as shown in Figure 3, where the antenna is represented with its Thevenin equivalent circuit. In Figure 3, $Z_a = R_a + jX_a$ is the complex antenna impedance, and $Z_c = R_c + jX_c$ is the complex chip (load) impedance. The antenna impedance is typically matched to the high-impedance state of the chip, in order to maximize the collected power.

An RFID chip is a nonlinear load, the complex impedance of which in each state varies with the frequency and the input power. The chip circuitry needs a certain minimum voltage or power to turn on. This threshold, and the impedance dependence on the input power, are determined by the details of the chip's RF front end, and by the power consumption of the specific chip [19]. The impedance dependence on the frequency is mostly determined by the chip's parasitic and packaging effects.

The variation of the chip's impedance with power and frequency can drastically affect the performance of the tag. Usually, the antenna impedance is matched to the chip's impedance at the minimum power level required for the chip to work, in order to maximize the tag's range. In most tag application scenarios, the tag continues to operate when brought closer to the RFID reader antenna, where the power incident on the tag is higher. However, it is possible to have a situation where a significant variation of the chip's impedance with a higher input power results in a severe tag impedance mismatch, and causes dead spots within the operational range of the tag.

4. Radar Cross Section of an RFID Tag

Let us understand how an RFID tag's radar cross section can be derived from the circuit shown in Figure 3. Although this circuit has some limitations, recently discussed in the literature [20-25], it can still be successfully applied to various antenna problems [26, 27]. Below, we show that this simple circuit can be used for calculating the power backscattered by tags with so-called minimum-scattering antennas [28-30], which represent a large class of RFID-tag antennas. Our results are consistent with findings by other authors.

The power scattered back from a loaded antenna can be divided into two parts. The first part is called the "structural mode," and is due to currents induced on the antenna when it is terminated with the complex-conjugate impedance. The second part is called the "antenna mode," and is due to the mismatch between the antenna's impedance and the load impedance [10, 15, 16]. This is the approach taken in [8] for the RCS derivation for an RFID tag.

The total backscattered field can also be written as the field scattered by the open-circuited antenna plus the re-radiated field [12]. The re-radiated power can be obtained from the equivalent circuit shown in Figure 3. This is the approach that we take to derive an RCS for an RFID tag. According to the circuit in Figure 3, an open-circuited antenna does not re-radiate any power. This holds true for minimum-scattering antennas. An antenna that is not a minimum-scattering antenna may still scatter back some power. However, for many antennas used in UHF RFID tags, this amount is typically small compared to the power scattered back by the same antenna terminated with the complex-conjugate-matched load (such as an RFID chip in its high-impedance state).

The power density of an electromagnetic wave incident on the RFID-tag antenna in free space is given by

$$S = \frac{P_t G_t}{4\pi r^2}, \tag{1}$$

where P_t is the transmitted power, G_t is the gain of the transmitting antenna, and r is the distance to the tag. The power, P_a, collected by the tag's antenna is by definition the maximum power that can be delivered to the complex-conjugate-matched load:

$$P_a = SA_e, \tag{2}$$

A_e is the effective area of the antenna, given by

$$A_e = \frac{\lambda^2}{4\pi} G, \tag{3}$$

and G is the tag antenna's gain. The power re-radiated by an RFID tag in the direction of the transmitter can be found from the circuit shown in Figure 3. It is the power dissipated in the antenna resistance, multiplied by the tag antenna's gain:

$$P_{re-radiated} = KP_a G\,, \tag{4}$$

where the factor K is given by

$$K = \frac{4R_a^2}{|Z_a + Z_c|^2}\,. \tag{5}$$

Equation (5) defines the influence of the load-impedance mismatch on the amount of re-radiated power. For example, an antenna loaded with a complex-conjugate impedance load re-radiates the same amount of power as the load absorbs. Table 1 gives values of the factor K for several values of antenna-load impedances.

From Table 1, one can see that when the antenna impedance is real, a short-circuited antenna re-radiates back four times as much power as the matched antenna [15, 8]. However, when the antenna impedance becomes sufficiently reactive ($|X_a/R_a| > \sqrt{3}$), the complex-conjugate-loaded antenna may re-radiate back more power than the short-circuited antenna, as illustrated in Figure 4.

For a minimum-scattering-tag antenna, the backscattered power is given by Equation (4). The radar cross section of the RFID tag can then be calculated as

$$\sigma = \frac{P_{re-radiated}}{S} = KA_e G\,. \tag{6}$$

Expressing the effective area of the antenna from Equation (3) and using the expression for the factor K from Equation (5), we can write the tag RCS as

$$\sigma = \frac{\lambda^2 G^2 R_a^2}{\pi |Z_a + Z_c|^2}\,. \tag{7}$$

This expression is derived directly from the simple equivalent circuit shown in Figure 3, and agrees with the RCS of the antenna loaded with an arbitrary load derived by other researchers [9, 15]. It is important to remember that the chip impedance in Equations (5) and (7) depends on the frequency and the input power. Equation (7) is valid for the reader and tag antennas with matched polarizations. In general, an RFID-tag RCS also depends on the polarization mismatch between the reader and the tag antennas [31].

It should be noted that the power of the modulated backscattered signal received by the RFID reader depends not only on the scalar difference between the radar cross sections defined by the two states of the tag chip's input impedance, but also on the relative phases of the reflected field components [32]. Two chip impedance states with equal scalar values of tag RCS may result in nonzero modulated backscattered signal power. The constant backscattered-field component due to scattering from an open-circuited antenna does not depend on the antenna's load, and has no effect on the power of the differential modulated signal received by an RFID reader [18].

Table 1. The K factor for different antenna load impedances.

Z_c	K
0	$\frac{4R_a^2}{R_a^2 + X_a^2}$
Z_a^*	1
∞	0

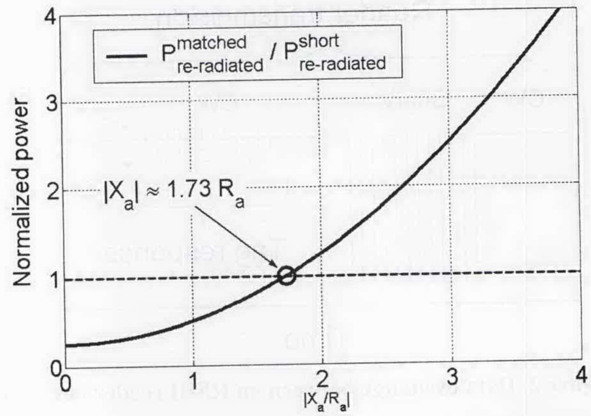

Figure 4. The power re-radiated by a complex-conjugate-matched antenna, normalized by the power re-radiated by the same antenna when it is short-circuited, as a function of the absolute value of the antenna's reactance-to-resistance ratio.

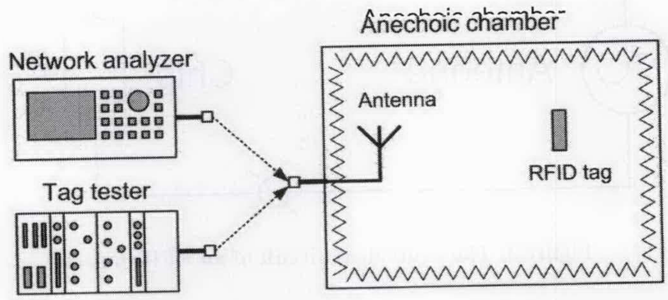

Figure 5. The experimental setup for measuring the radar cross section of an RFID tag.

5. Measurement Methodology

There exist various techniques for measuring the radar cross section of loaded antennas. These techniques typically involve separate transmitting and receiving antennas and complex RF hardware, including decoupling equipment or a two-port automatic network analyzer [16, 33-35]. We propose a simple method of measuring the radar cross section of an RFID tag using the experimental setup shown in Figure 5. The method is based on a single-port network-analyzer measurement.

The return loss of the transmitting antenna is first measured with the network analyzer for an empty anechoic chamber, without an RFID tag. The measured value includes the effects of input-port mismatch and internal reflections inside the anechoic chamber. It is used as a reference level, and is subtracted from the return loss measured in the presence of the tag. This standard background-subtraction procedure in RCS measurements allows us to calculate the backscattered power and to find the tag's RCS. We used the RFID tag tester to determine the minimum power level necessary for the RFID tag to turn on.

The return loss measured after the background subtraction can be approximated as

$$|S_{11}|^2 \approx \frac{P_{received}}{P_t}, \tag{8}$$

where $P_{received}$ is the power backscattered from the tag and received by the network analyzer. In the anechoic chamber, it can be calculated from the classical radar equation [36] as

$$P_{received} = \frac{P_t G_t^2 \lambda^2 \sigma}{(4\pi)^3 r^4}. \tag{9}$$

Using Equations (8) and (9), the RFID-tag cross section can be calculated from the measured return loss as

$$\sigma = |S_{11}|^2 \frac{(4\pi)^3 r^4}{G_t^2 \lambda^2}. \tag{10}$$

For our measurements, we used the RFID tag in the form of a small meandered dipole, etched in 0.5 oz copper on a 2 mil polyester substrate with a dielectric permittivity of 3.5. The RFID chip was mounted directly on the antenna terminals using flip-chip packaging. This tag was similar to the one used as an example in [5], but with the loading bar removed to minimize the scattering from an open-circuited antenna. Photographs of the three antenna samples used in the measurements (chip-loaded, open-circuited, and short-circuited) are shown in Figure 6.

For measurement equipment, we used a standard network analyzer, HP8719C, with an output power level limited to 10 dBm. We also used the tag tester, which was built on a National Instruments modular hardware platform, and had the same basic architecture as the RFID reader shown in Figure 1. It consisted of a PXI-5671 RF vector signal generator, a PXI-5660 RF signal analyzer, a PXI-8196 computer controller running *LabVIEW*, a power amplifier, and a circulator. We developed a *LabVIEW* application that generated query commands with desired modulation and coding formats for RFID UHF tags operating under ISO and Gen2 protocols. The commands were sent at specified frequencies. The output

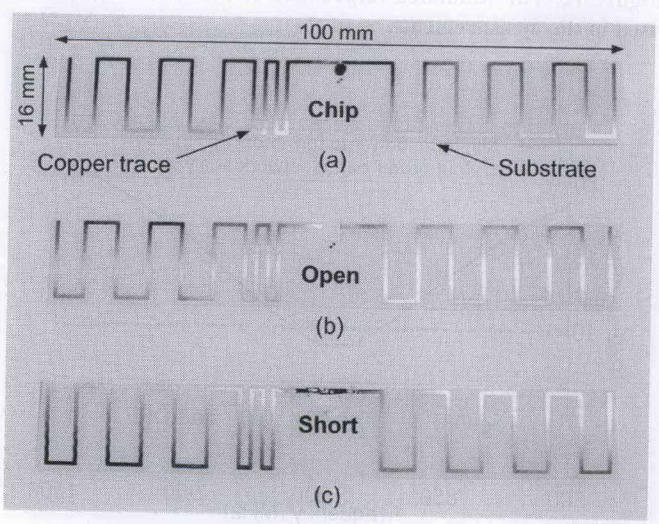

Figure 6. Samples of RFID-tag antennas, used in the measurements: (a) chip-loaded, (b) open-circuited, and (c) short-circuited.

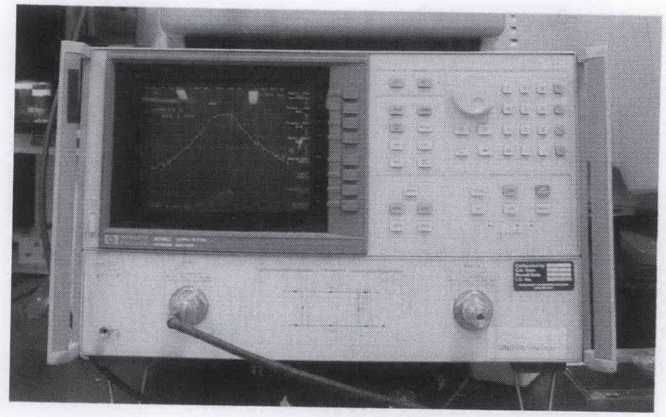

Figure 7. The network analyzer.

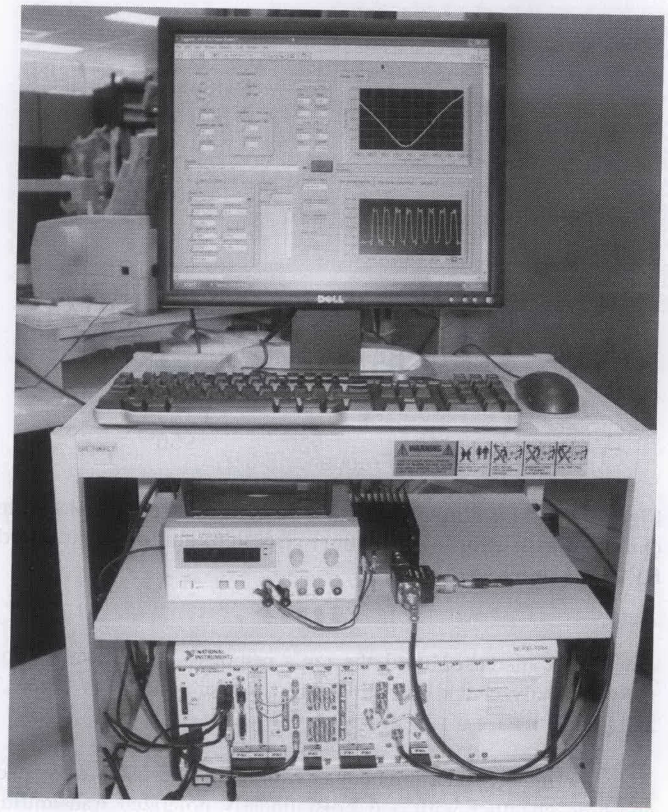

Figure 8. The RFID tag tester.

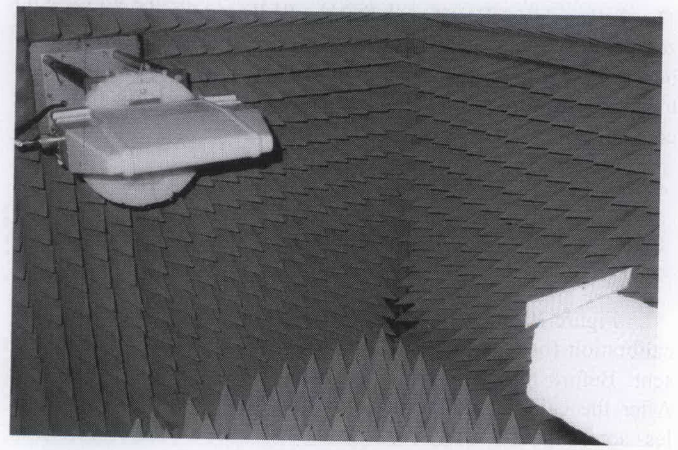

Figure 9. The anechoic chamber, with the transmitting antenna and the RFID tag.

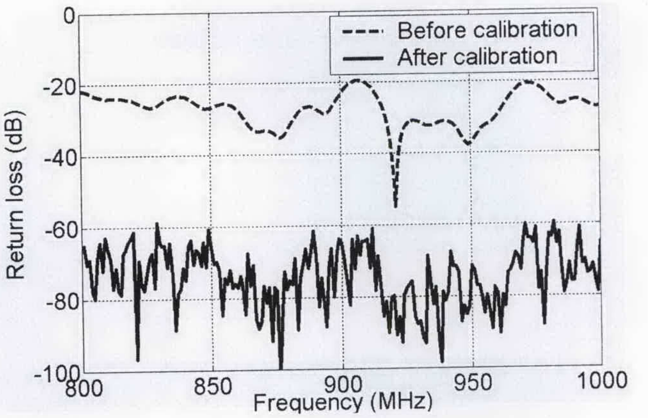

Figure 10. The antenna return loss, measured in an empty anechoic chamber, before and after calibration.

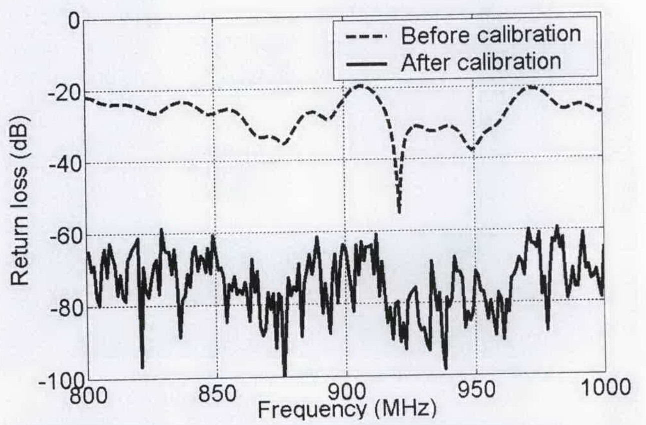

Figure 11. The Antenna return loss, measured in anechoic chamber with chip-loaded, short-circuited, and open-circuited RFID-tag antennas.

power was increased until the tag's response was detected. The network analyzer and the RFID tag tester are shown in Figure 7 and Figure 8.

For the RF measurement environment, we used a compact anechoic chamber with a 6.2 dBi linearly polarized transmitting antenna and a foam stand for the tag. The tag was located at a distance of approximately 0.5 m away from the transmitting antenna. The distance was chosen such that the RFID tag was in the far-field zone, but received sufficient power to turn on. The anechoic chamber is shown in Figure 9. The transmitting antenna was connected to either the network analyzer or the tag tester with a 3 m long coaxial cable.

6. Results

Figure 10 shows the measured return loss before and after calibration (background subtraction), when no RFID tag was present. Before the calibration, the return loss was –20 dB or less. After the calibration, the background noise level was –60 dB or less across the frequency band.

Figure 11 presents the measured return loss after calibration for chip-loaded, short-circuited, and open-circuited tag antennas. One can see that the open-circuited dipole antenna was not an ideal minimum-scattering antenna, as it still backscattered some power above the background noise level [16]. However, this amount was small, and was less than the power scattered back by a short-circuited antenna. This agreed with the theoretical results given in Table 1.

We observed that the tag antenna loaded with the chip scattered back more power than the short-circuited antenna. For example, at the resonant frequency of 890 MHz, the observed difference was approximately 15 dB. This was due to the fact that the antenna's impedance in the frequency band of interest (800-1000 MHz) was highly reactive. The absolute value of reactance-to-resistance ratio was $|X_a/R_a| > 5$ for all frequencies. This can be seen from Figure 12, which presents the plot of antenna impedance as a function of frequency obtained from the electromagnetic simulations using Method of Moments software (Ansoft *Designer*).

The output power level of the network analyzer was limited to 10 dBm, at which all RCS measurements were performed. The tag was not turned on for all frequencies in Figure 11. The minimum power necessary to turn the tag on inside the anechoic chamber was determined with the tag tester. This power is plotted in Figure 13, in comparison with the output power of the network analyzer. One can see that the RFID tag received sufficient power to become energized and turn on only for the frequencies between

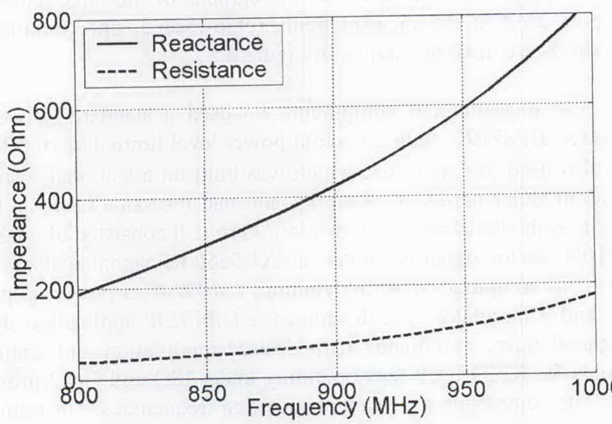

Figure 12. The simulated impedance of the RFID-tag antenna used in the measurements.

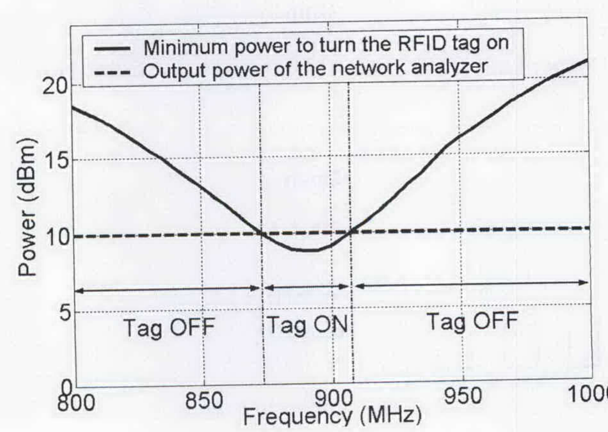

Figure 13. The minimum power necessary to turn on the RFID tag in the anechoic chamber, compared to the output power level of the network analyzer.

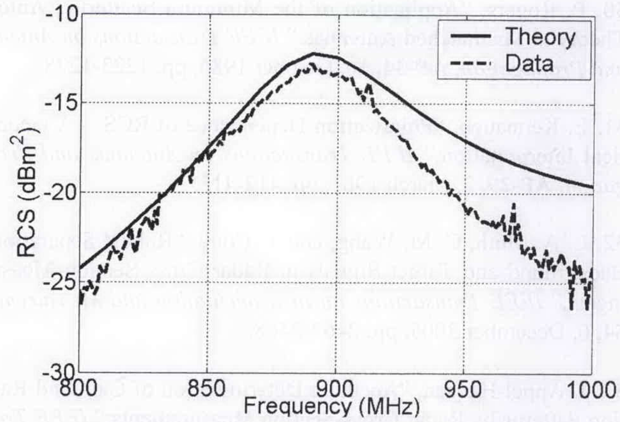

Figure 14. The theoretical and measured values of the RFID tag's radar cross section.

approximately 875 MHz and 905 MHz. The minimum power plotted in Figure 13 can be used to calculate the RFID tag's range [5].

Figure 14 shows theoretical and measured RCS values for the chip-loaded RFID tag antenna shown in Figure 6a. The theoretical radar cross section was calculated from Equation (7), where the tag's antenna impedance and gain were obtained from electromagnetic simulations, and the chip impedance was measured experimentally. The chip-loaded RFID tag resonated in free-space at a frequency of approximately 890 MHz, where the antenna gain was 1.8 dBi and the antenna impedance was $70+j400$ ohms. The chip's impedance (high-impedance state) was measured to be $12-j400$ ohms at that frequency for the power level in the experiment. The experimentally measured RCS was obtained from Equation (10).

The peak theoretical value of RCS for the RFID tag was approximately –12.5 dBsqm at 890 MHz, which agreed reasonably well with the experimentally measured RCS. The observed differences across the band were most likely due in part to inaccuracy in the measurement of the chip's impedance as a function of power and frequency, in part to the polarization mismatch caused by antenna misalignment, and in part to errors in determining the exact distance between the small tag antenna and the large transmitting antenna.

RCS measurements of RFID tags using our method can also be performed in other RF environments, such as a GTEM cell, where an appropriate theoretical formulation must be used to relate the measured return loss to the tag's radar cross section.

7. Summary

We presented a theory for an RFID tag's radar cross section. We described an experimental method of measuring a tag's RCS using a single-port network analyzer, connected to an antenna in an anechoic chamber with the tag inside. Measurements were performed using an RFID tag operating in the UHF band. The theoretical results agreed well with experimental data.

8. References

1. J. Landt, "The History of RFID," *IEEE Potentials*, **24**, 4, October-November 2005, pp. 8-11.

2. A. R. Koelle, S. W. Depp, and R. W. Freyman, "Short-Range Radio-Telemetry for Electronic Identification, Using Modulated RF Backscatter," *Proceedings of the IEEE*, **63**, 8, August 1975, pp. 1260-1261.

3. A. R. Koelle, "Short Range UHF Telemetry System Using Passive Transponders for Vehicle ID and Status Information," IEEE Workshop on Automotive Applications of Electronics, October 1988, pp. 34-38.

4. R. Want, "An Introduction to RFID Technology," *IEEE Pervasive Computing*, **5**, 1, January-March 2006, pp. 25-33.

5. K. V. S. Rao, P. V. Nikitin, and S. F. Lam, "Antenna Design for UHF RFID Tags: A Review and a Practical Application," *IEEE Transactions on Antennas and Propagation*, **AP-53**, 12, December 2005, pp. 3870 -3876.

6. P. V. Nikitin and K. V. S. Rao, "Measurement of Backscattering from RFID Tags," *Proceedings of Antennas Measurement Techniques Association Symposium*, Newport, RI, October 2005.

7. Hongil Kwon and Bomson Lee, "Meander Line RFID Tag at UHF Band Evaluated with Radar Cross Sections," *Asia-Pacific Microwave Conference Proceedings*, **4**, December 2005, pp. 1-4.

8. K. Penttila, M. Keskilammi, L. Sydanheimo, and M. Kivikoski, "Radar Cross-Section Analysis for Passive RFID Systems," *IEE Proceedings on Microwaves, Antennas and Propagation*, **153**, 1, February 2006, pp. 103-109.

9. R. Harrington, "Electromagnetic Scattering by Antennas," *IEEE Transactions on Antennas and Propagation*, **AP-11**, 5, September 1963, pp. 595-596.

10. J. Wang, C. Chang, and R. Moore, "Precision Experimental Characterization of the Scattering and Radiation Properties of Antennas," *IEEE Transactions on Antennas and Propagation*, **AP-30**, 1, January 1982, pp. 108-112.

11. R. Janaswamy and Shung-Wu Lee, "Scattering from Dipoles Loaded with Diodes," *IEEE Transactions on Antennas and Propagation*, **AP-36**, 11, November 1988, pp. 1649-1651.

12. R. C. Hansen, "Relationships Between Antennas as Scatterers and as Radiators," *Proceedings of the IEEE*, **77**, 5, May 1989, pp. 659-662.

13. Chien-Chang Huang and Tah-Hsiung Chu, "Analysis of Wire Scatterers with Nonlinear or Time-Harmonic Loads in the Frequency Domain," *IEEE Transactions on Antennas and Propagation*, **AP-41**, 1, January 1993, pp. 25-30.

14. J. T. Mayhan, A. R. Dion, and A. J. Simmons, "A Technique for Measuring Antenna Drive Port Impedance Using Backscatter Data," *IEEE Transactions on Antennas and Propagation*, **AP-42**, 4, April 1994, pp. 526-533.

15. K. Schneider, "A Re-Look at Antenna In-Band RCSR via Load Mismatching," IEEE International Symposium on Antennas and Propagation *Digest*, **2**, June 1996, pp. 1398-1401.

16. W. Wiesbeck and E. Heidrich, "Wide-Band Multiport Antenna Characterization by Polarimetric RCS Measurements," *IEEE Transactions on Antennas and Propagation*, **AP-46**, 3, March 1998, pp. 341-350.

17. R. Glidden, et al., "Design of Ultra-Low-Cost UHF RFID Tags for Supply Chain Applications," *IEEE Communications Magazine*, **42**, 8, August 2004, pp. 140-151.

18. J.-P. Curty, N. Joehl, C. Dehollain, and M. J. Declercq, "Remotely Powered Addressable UHF RFID Integrated System," *IEEE Journal of Solid-State Circuits*, **40**, 11, November 2005, pp. 2193-2202.

19. G. De Vita and G. Iannaccone, "Design Criteria for the RF Section of UHF and Microwave Passive RFID Transponders," *IEEE Transactions on Microwave Theory and Techniques*, **MTT-53**, 9, September 2005, pp. 2978-2990.

20. J. Van Bladel, "On the Equivalent Circuit of a Receiving Antenna," *IEEE Antennas and Propagation Magazine*, **44**, 1, February 2002, pp. 164-165.

21. R. E. Collin, "Limitations of the Thevenin and Norton Equivalent Circuits for a Receiving Antenna," *IEEE Antennas and Propagation Magazine*, **45**, 2, April 2003, pp. 119-124.

22. J. B. Andersen and R. G. Vaughan, "Transmitting, Receiving, and Scattering Properties of Antennas," *IEEE Antennas and Propagation Magazine*, **45**, 4, August 2003, pp. 93-98.

23. A. W. Love, "Comment on 'Limitations of the Thevenin and Norton Equivalent Circuits for a Receiving Antenna'," *IEEE Antennas and Propagation Magazine*, **45**, 4, August 2003, pp. 98-99.

24. D. Pozar, "Scattered and Absorbed Powers in Receiving Antennas," *IEEE Antennas and Propagation Magazine*, **46**, 1, February 2004, pp. 144-145.

25. W. Geyi, "Derivation of Equivalent Circuits for Receiving Antenna," *IEEE Transactions on Antennas and Propagation*, **AP-52**, 6, June 2004, pp. 1620-1623.

26. J. Reale, "The Receive Voltage Transmission Function of a Phased Array Antenna Element," *IEEE Transactions on Antennas and Propagation*, **AP-25**, 4, July 1977, pp. 542-547.

27. M. Sato and R. Sato, "Analysis of Transient Responses Between Coupled Dipole Antennas by Using a Simple Equivalent Circuit," *IEEE Transactions on Antennas and Propagation*, **AP-33**, 9, September 1985, pp. 1015-1020.

28. W. Kahn and H. Kurss, "Minimum-Scattering Antennas," *IEEE Transactions on Antennas and Propagation*, **AP-13**, 5, September 1965, pp. 671-675.

29. W. Wasylkiwskyj and W. Kahn, "Theory of Mutual Coupling Among Minimum-Scattering Antennas," *IEEE Transactions on Antennas and Propagation*, **AP-18**, 2, March 1970, pp. 204-216.

30. P. Rogers, "Application of the Minimum Scattering Antenna Theory to Mismatched Antennas," *IEEE Transactions on Antennas and Propagation*, **AP-34**, 10, October 1986, pp. 1223-1228.

31. E. Kennaugh, "Polarization Dependence of RCS – A Geometrical Interpretation," *IEEE Transactions on Antennas and Propagation*, **AP-29**, 2, March 1981, pp. 412-413.

32. L. A. Muth, C. M. Wang, and T. Conn, "Robust Separation of Background and Target Signals in Radar Cross Section Measurements," *IEEE Transactions on Instrumentation and Measurement*, **54**, 6, December 2005, pp. 2462-2468.

33. J. Appel-Hansen, "Accurate Determination of Gain and Radiation Patterns by Radar Cross-Section Measurements," *IEEE Transactions on Antennas and Propagation*, **AP-27**, 5, September 1979, pp. 640-646.

34. J. F. Lindsey, "Radar Cross-Section Effects Relating to a Horn Antenna," *IEEE Transactions on Antennas and Propagation*, **AP-37**, 2, February 1989, pp. 257-260.

35. W. Weir, L. Robinson, and D. Parker, "Broadband Automated Radar Cross Section Measurements," *IEEE Transactions on Antennas and Propagation*, **AP-22**, 6, November 1974, pp. 780-784.

36. M. O. White, "Radar Cross-Section: Measurement, Prediction, Control," *Electronics and Communication Engineering Journal*, **10**, 4, August 1998, pp. 169-180.

9. Acknowledgements

The authors would like to thank their colleagues, Dr. Rene Martinez, Dr. Harley Heinrich, Mr. Vijay Pillai, and Mr. Sander Lam, for their valuable suggestions and discussions.

Introducing the Authors

Pavel V. Nikitin is a Lead Engineer working at Intermec Technologies Corporation, Everett, WA, where he is actively involved with the design and development of antennas for RFID tags. He has authored over 40 technical publications in journals and conferences, and has several US patents pending. Dr. Nikitin graduated from Utah State University with a BSEE and an MSEE in 1994 and 1998, respectively; from Novosibirsk State University, Novosibirsk, Russia, with a BS in Physics in 1995; and from Carnegie-Mellon University with a PhD degree in Electrical and Computer Engineering in 2002. His experience includes work at Ansoft and IBM Corporations and a postdoctoral position at the University of Washington. He is a Member of the IEEE.

K. V. Seshagiri Rao is a Technologist with Intermec Technologies Corporation, where he also manages a group in the area of RFID transponder design and development. He coauthored the book *Millimeter-Wave Microstrip and Printed Circuit Antennas* (Artech House, 1991), and approximately 35 technical publications in journals and conferences. He also has 13 US patents in the area of RFID. Dr. Rao received the PhD degree from the Indian Institute of Technology, Kharagpur, India, in 1984. His experience includes a faculty position at the Indian Institute of Technology; a postdoctoral position at the University of Ottawa, Ottawa, ON, Canada; and work at Antenna Research Associates and IBM. He is a Senior Member of the IEEE.